

Controlled generation and steering of spatial gap solitons

Dragomir Neshev,¹ Andrey A. Sukhorukov,¹ Brendan Hanna,² Wieslaw Krolikowski,² and Yuri S. Kivshar¹

¹*Nonlinear Physics Group and Centre for Ultra-high bandwidth Devices for Optical Systems (CUDOS),
Research School of Physical Sciences and Engineering,
Australian National University, Canberra, ACT 0200, Australia**

²*Laser Physics Center and Centre for Ultra-high bandwidth Devices for Optical Systems (CUDOS),
Research School of Physical Sciences and Engineering,
Australian National University, Canberra, ACT 0200, Australia*

We demonstrate the first fully controlled generation of *immobile and slow spatial gap solitons* in nonlinear periodic systems with band-gap spectra, and reveal the key features of gap solitons which distinguish them from conventional counterparts, including a dynamical transformation of gap solitons due to *nonlinear inter-band coupling*. We also predict theoretically and confirm experimentally the effect of *anomalous steering* of gap solitons in optically-induced photonic lattices.

PACS numbers: 42.65.Tg, 42.65.Jx, 42.70.Qs

Nonlinear wave self-action plays an important role in many physical systems ranging from water waves to optical beams and Bose-Einstein condensates (BECs). Nonlinearity can suppress wave spreading leading to the formation of *solitary waves* which, due to their robustness, can find many applications, e.g. in long-distance communication systems. Almost two decades ago, it was suggested that the systems with periodically modulated parameters can support a novel type of solitons—*gap solitons*, which may exist in band gaps of the linear spectra due to strong wave scattering and coupling between the forward and backward propagating waves [1, 2]. It was predicted that gap solitons may exist in different nonlinear periodic structures including fiber Bragg gratings [3], two- and three-dimensional photonic crystals [4], and BEC in optical lattices [5].

According to the theoretical predictions, gap solitons have many unique properties, which distinguish them from conventional solitons [3]: (i) they can form in both self-focusing and self-defocusing nonlinear media; (ii) soliton velocity and dispersion are nontrivially modified; (iii) the gap solitons become unstable and undergo dynamical transformations above a critical amplitude due to the inter-band resonances [6, 7]. For gap solitons observed experimentally in fiber Bragg gratings [8] and waveguide arrays [9], only some reduction of the soliton velocity was observed. This has prevented an experimental study of dispersion properties of gap solitons and associated band-gap effects, since such effects become evident for slow and immobile solitons only.

In this Letter, we demonstrate the first fully controlled generation of spatial gap solitons where the soliton power and velocity may be independently varied. In particular, we observe experimentally *immobile gap solitons*. We demonstrate the gap-soliton steering, reveal their unusual mobility, and observe, for the first time to our knowledge, the gap-soliton dynamics due to instability development. Our experimental results are in excellent agreement with the key theoretical predictions, underlying generic prop-

erties of gap solitons with implications to a variety of nonlinear periodic systems beyond the field of optics.

We investigate the gap-soliton formation in photonic lattices created by interfering ordinary polarized laser beams in a biased photorefractive crystal. *Discrete solitons* in such lattices were observed recently [10, 11]; this allows us to compare two types of solitons emphasizing the intriguing properties of gap solitons.

First, we determine the optimal conditions for gap-soliton generation, using the normalized paraxial equation for the probe beam electric field envelope $E(x, z)$,

$$i\frac{\partial E}{\partial z} + D\frac{\partial^2 E}{\partial x^2} + \mathcal{F}(x, |E|^2)E = 0, \quad (1)$$

where x and z are the transverse and propagation coordinates, normalized to the characteristic values x_0 and z_0 , respectively, $D = z_0\lambda/(4\pi n_0 x_0^2)$ is the beam diffraction coefficient, n_0 is the average medium refractive index, and λ is the vacuum wavelength. The optically induced change of the refractive index is [10, 11]

$$\mathcal{F}(x, |E|^2) = -\gamma(I_b + I_p(x) + |E|^2)^{-1}, \quad (2)$$

where I_b is the constant dark irradiance, $I_p(x)$ is the two-beam interference pattern which induces the periodic lattice with a period d ,

$$I_p(x) = I_g \cos^2(\pi x/d), \quad (3)$$

and γ is a nonlinear coefficient proportional to the applied DC field. In order to match our experimental conditions, we use below the following parameters for the theory and numerical calculations: $\lambda = 0.532 \mu\text{m}$, $n_0 = 2.4$, $x_0 = 1 \mu\text{m}$, $z_0 = 1\text{mm}$, $d = 22.2$, $I_b = 1$, $I_g = 1$, $\gamma = 5.31$, the crystal length is $L = 15 \text{ mm}$. We note that the model Eq. (1) is very general and appears in other areas of physics. It can describe, in particular, the BEC dynamics in optical lattices where the matter-wave gap solitons are expected to have similar properties to optical counterparts.

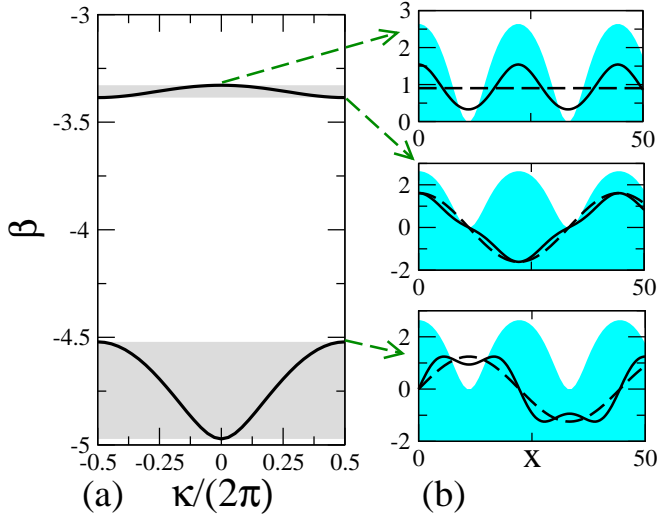


FIG. 1: (a) Dispersion of Bloch waves in an optically-induced lattice; the spectrum bands are shaded. (b) Bloch-wave profiles (solid) and leading-order Fourier components (dashed) superimposed on top of the normalized refracted index profile of the periodic lattice (shown with shading) for different gap edges indicated by the arrows.

Existence of spatial bright solitons is closely linked to the structure of the linear wave spectrum. In periodic lattices, the spectrum is composed of bands corresponding to the propagating *Floquet-Bloch modes*, which are separated by gaps where the wave propagation is forbidden. The Floquet-Bloch modes are solutions of linearized Eq. (1) in the form $E_{\kappa,n}(x, z) = \psi_{\kappa,n}(x) \exp(i\kappa x/d + i\beta_{\kappa,n}z)$, where $\beta_{\kappa,n}$ and κ are the Bloch-wave propagation constant and wavenumber, respectively, and the index $n = 1, 2, \dots$ marks the order of the transmission band. The Bloch wave $\psi_{\kappa,n}(x)$ has the periodicity of the photonic structure, $\psi_{\kappa,n}(x + d) \equiv \psi_{\kappa,n}(x)$, and this condition defines the dispersion relation $\beta_{\kappa,n}$, as sketched in Fig. 1(a). The open regions in this plot mark band gaps where $\text{Im}\kappa \neq 0$: the top one exists due to total internal reflection and extends to $\beta \rightarrow +\infty$, whereas lower gaps have a finite width and appear due to Bragg scattering from the periodic structure.

In order to underline the essential physics of the soliton formation in periodic lattices, first we consider the small-amplitude limit. We seek solutions of Eq. (1) near the band edge in the form of modulated Bloch waves, $E = \varphi(x, z)\psi_{\kappa,n} \exp(i\beta_{\kappa,n}z + i\kappa x/d)$, and derive the nonlinear Schrödinger equations for the slowly varying Bloch-wave envelope [12],

$$i \frac{\partial \varphi}{\partial z} + iV_g \frac{\partial \varphi}{\partial x} + \frac{\eta}{2} \frac{\partial^2 \varphi}{\partial x^2} + \Gamma |\varphi|^2 \varphi = 0. \quad (4)$$

Here $V_g = -d \partial \beta / \partial \kappa|_{\beta_{\kappa,n}}$ is the group velocity, $\eta = -d^2 \partial^2 \beta / \partial \kappa^2|_{\beta_{\kappa,n}}$ is the effective diffraction coefficient, and $\Gamma = \int_0^d [\mathcal{F}(x, |\psi_{\kappa,n}|^2) - \mathcal{F}(x, 0)] |\psi_{\kappa,n}|^2 dx$ is the

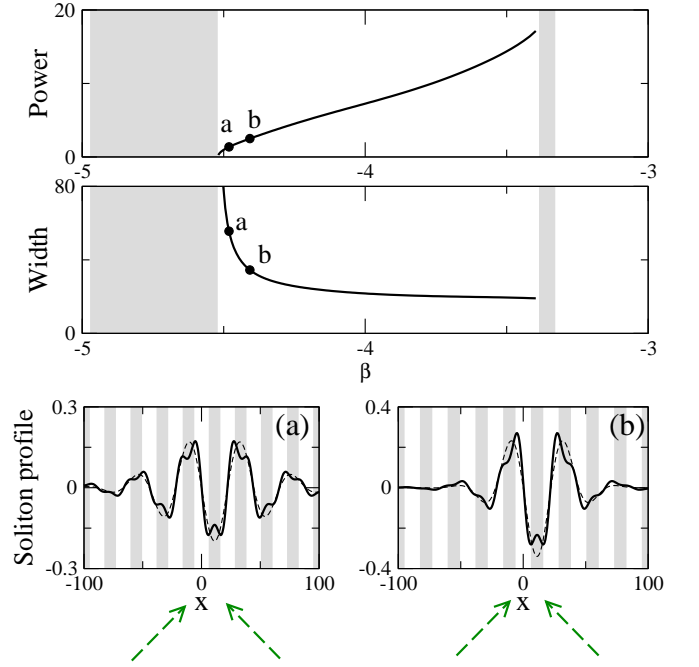


FIG. 2: Numerical results for a gap soliton family: Power (top) and width (middle) vs. the propagation constant. Bottom: soliton profiles (solid) corresponding to the marked points (a) and (b) in the upper plots; shadings mark the grating minima. Arrows illustrate schematically the direction of the input beams, which interference pattern (shown with dashed line) approximates the soliton profile.

effective nonlinear coefficient, where we assume the normalization $\int_0^d |\psi_{\kappa,n}|^2 dx \equiv 1$. Equation (4) possesses localized solutions for bright solitons, $\varphi = \sqrt{2\rho/\Gamma} \text{sech}[(x - V_g z)\sqrt{\rho/\eta}] \exp(i\rho z)$, provided $\eta\Gamma > 0$ and ρ is a free parameter. Thus, for self-focusing medium nonlinearity ($\Gamma > 0$), the gap solitons appear near the lower-gap edges of the bandgap spectrum.

Next, we find soliton solutions of the full model Eqs. (1)-(3), shown in Fig. 2, and identify a number of important differences between the conventional and gap solitons which appear when the propagation constant is shifted deep inside the gap, where the envelope approximation (4) is no longer valid. Specifically, the power of gap solitons is bounded from above [Fig. 2(top)], and their width is bounded from below [Fig. 2(middle)]. These limitations appear because the Bragg-reflection gap always has a finite width, in contrast to the semi-infinite gap where conventional (or discrete) solitons are localized.

Controlled experimental excitation of spatial gap solitons can be realized if the modulated Bloch-wave profile is properly matched at the input. Since the Bloch waves are periodic, they can be decomposed into the Fourier series, $\psi_{\kappa,n} = \sum_m C_n(\kappa + 2\pi m) \exp[ix(\kappa + 2\pi m)/d]$. In Fig. 1(b) we show the characteristic profiles of the Bloch

waves, and also plot the contribution from the leading-order Fourier components (dashed lines). We find that in the leading order $\psi_{0,1} = C_1(0) + \dots$, therefore lattice solitons in the semi-infinite total internal reflection gap can be generated by a *single incident beam*, as was realized in earlier experiments for arrays of weakly coupled optical waveguides. On the contrary, the Bloch waves in the Bragg-reflection gap are composed of the *counter-propagating waves*, e.g. $\psi_{\pi,n} = C_n(\pi)\exp(i\pi x/d) + C_n(-\pi)\exp(-i\pi x/d) + \dots$ for $n = 1, 2$. Therefore, spatial gap solitons can be generated by using *two Gaussian beams* which are tuned to the Bragg resonance and have opposite inclination angles, as was originally suggested in Ref. [13] and developed further in Ref. [7]. Therefore, we consider the input electric field in the form,

$$E_0(x) = \sqrt{I_0}e^{-(x-x_e)^2/w^2} \cos[\pi(x-x_s)/d], \quad (5)$$

where the exponential term approximates the gap soliton envelope, w being the width of the input beams, and the interference term approximates the Bloch-wave profile, with the shift x_s depending on the relative phase difference between the two beams, and we choose $x_e = d/2$ and $w = 55$. When the interference maxima are at the minima of the refractive index profile, the Bloch mode is excited at the lower edge of the Bragg-reflection gap, and the input pattern can match very closely the gap-soliton profile, as shown in examples of Figs. 2(a,b).

We investigated numerically the dynamics of the two-beam mutual focusing and the gap-soliton generation by simulating the model Eq. (1) with the input condition (5) chosen to match the Bloch-wave profile at the lower gap edge. The beams diffract at a low input power [Fig. 3(a)], whereas an immobile gap soliton forms when the input power is increased [Fig. 3(b)]. We note that the required power depends on the input beam width, as follows from Fig. 2, and the minimum soliton width defines a fundamental limitation of the degree of two-beam mutual focusing. Indeed, as the power is increased, an instability rapidly develops through a resonant excitation of the first band, and subsequent formation of a quasi-periodic breather [Fig. 3(c)]. Similar breathing states were recently observed in waveguide arrays [14].

Our experiments were performed in a 15mm-long Strontium Barium Niobate (SBN:60) crystal externally biased along the crystalline c -axis. The experimental setup is similar to that discussed in Ref. [11] with the difference that the extraordinary polarized probe beam was split into two parts which were later focused by cylindrical lens and made to overlap at the input face of the crystal. The angle between these two beams was set to twice the Bragg angle, such that the periodicity of the interference pattern is equal to that of the lattice ($22 \mu\text{m}$). In our case, such value of the periodicity allows for a relatively wide gap in the transmission spectrum, as shown in Fig. 1(a). The relative phase between the probe beams was tuned such that a symmetric interference pattern is

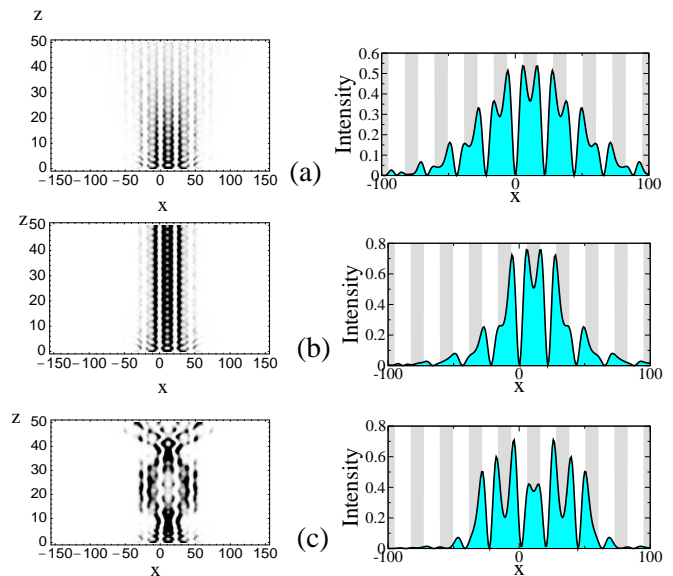


FIG. 3: Numerical results. Dynamics of the Bloch waves excited through two-beam interference: (a) linear diffraction at low power ($I_0 \simeq 0$), (b) excitation of a gap soliton in the nonlinear regime ($I_0 = 0.048$), (c) beam breakup and the formation of a quasi-periodic breathing state at higher powers ($I_0 = 0.28$). Left: variation of intensity along the propagation direction; Right: beam profiles at the crystal output ($z = 15\text{mm}$) normalized to I_0 .

obtained, as shown in Fig. 4(top). The relative position between this pattern and the lattice could also be controlled, by changing the relative phase between the two lattice forming beams [11]. The input width of the overlapping probe beams is $w = 55 \mu\text{m}$ ($65 \mu\text{m}$ FWHM), while they are fully separated at the output for zero bias field. When electric field of 5000 V/cm is applied to the crystal, the index grating (optical lattice) is formed and the probe beams excite Bloch waves in the first or the second band, depending on the relative lattice position.

The experimental results shown in Fig. 4 represent remarkably all theoretical predictions. First, we align the interference maxima of the input beams with the minima of the induced lattice at the input face of the crystal and record the beam profiles at back face for several input powers [see Fig. 4(left column)]. The output intensity is exactly zero at the maxima of the index grating. The intensity maxima are out-of-phase, as confirmed with interferometric measurements, and possess a double peak structure located at the minima of the grating. At low powers, the output intensity pattern is broad and corresponds to the Bloch waves at the lower gap edge. The beam is exactly centered between two unperturbed output beams [dashed curve in Fig. 4(left column, top plot)] measured for zero voltage. At higher intensity ($I_0/I_g = 0.04$), we observe mutual focusing, and self-trapping into a spatial gap soliton is observed at $I_0/I_g = 0.14$ [see Fig. 4(left column)]. The gener-

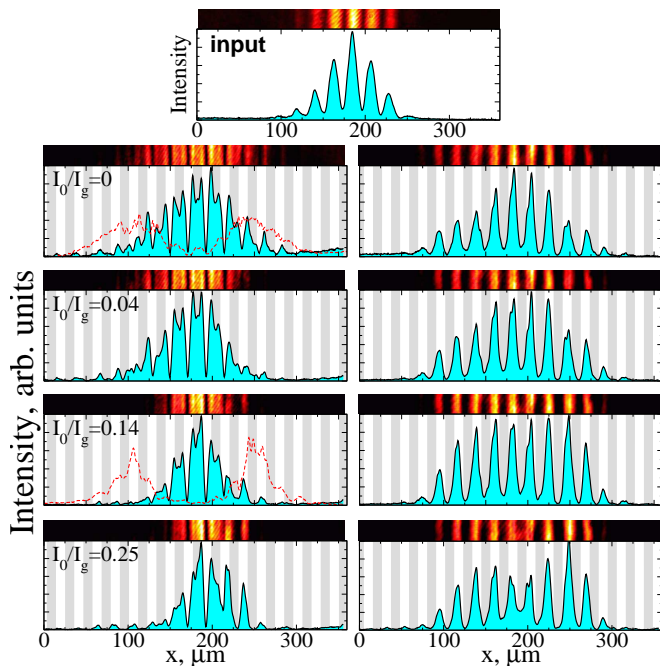


FIG. 4: Experimental results for two-beam interaction showing the intensity profiles at the crystal input (top) and output for varying beam power: Left: mutual focusing and gap soliton formation when interference maxima are aligned with the lattice minima; Right: self-defocusing when interference maxima of the input beams are at the lattice maxima. Dashed curves represent the beam profiles at the indicated beam intensity when the grating is erased.

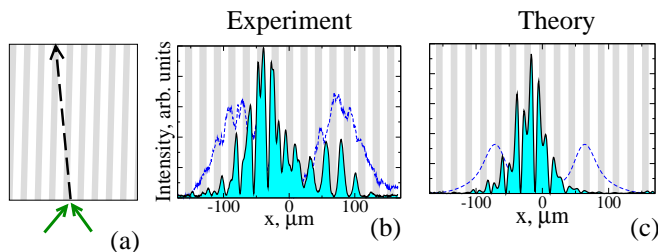


FIG. 5: (a) Schematic demonstration of anomalous gap-soliton steering induced by a tilt of the lattice; dashed line shows the propagation direction of a gap soliton; solid lines indicate the directions of the input beams. (b,c) Output soliton profile for a lattice tilt in the direction of larger x by 20% of the Bragg angle with respect to normal; dashed lines show the beam profiles when the lattice is absent.

ated gap soliton has zero transverse velocity, and is centered between the two output beams which separate if the grating is erased (dashed curve). As predicted theoretically, the effect of the mutual focusing is limited and at higher intensities ($I_0/I_g = 0.25$) the beam disintegrates [see Fig. 4(left column, bottom plot)] while its profile becomes asymmetric due to the diffusion contribution to the photorefractive nonlinearity. On the other

hand, when we align the interference maxima of the input beams to the lattice maxima, the excited Bloch wave corresponds to the upper gap edge [see Fig. 1] and they experience anomalous diffraction ($\eta < 0$) leading to self-defocusing as the power is increased [Fig. 4(right)].

Finally, we study mobility of spatial gap solitons and a possibility to vary their transverse velocity. Experimentally, the soliton motion is induced by tilting the lattice by 20% of the Bragg angle thus introducing a lateral shift of the induced waveguides by $16\mu\text{m}$ at the output [the lattice is shifted to the right in Fig. 5(a)]. Results of the experimental observations and the numerical simulations are presented side-by-side in Fig. 5(b,c) show that the generated gap solitons *move to the left* when the grating is *tilted to the right*. In experiment, on the right-hand side of the gap soliton, a small contribution from the first band is observed, which appears due to asymmetry in the initial excitation and inhomogeneities of the lattice. This *anomalous steering* behavior occurs because the spatial group-velocity dispersion for gap solitons is almost three times larger compared to a homogeneous crystal. This is in sharp contrast with conventional lattice (or discrete) solitons, that tend to propagate along the lattice [15].

In conclusion, we have demonstrated experimentally the first fully controlled generation of spatial gap solitons in optically-induced periodic photonic lattices and observed novel effects such as anomalous steering of gap solitons and the limitation of the two-beam mutual focusing through inter-band coupling. We believe our results can be useful for the study of nonlinear effects in photonic crystals and nonlinear dynamics of the Bose-Einstein condensates in optical lattices.

* URL: www.rsphysse.anu.edu.au/nonlinear

- [1] Yu. I. Voloshchenko *et al.*, Zh. Tekh. Fiz. **51**, 902 (1981) (in Russian) [Tech. Phys. **26**, 541 (1981)].
- [2] W. Chen and D.L. Mills, Phys. Rev. Lett. **58**, 160 (1987).
- [3] C. M. de Sterke and J. E. Sipe, in *Progress in Optics*, Vol. XXXIII, Ed. E. Wolf (North-Holland, Amsterdam, 1994), p. 203.
- [4] N. Akozbek and S. John, Phys. Rev. E **57**, 2287 (1998).
- [5] O. Zobay *et al.*, Phys. Rev. A **59**, 643 (1999).
- [6] I. V. Barashenkov *et al.*, Phys. Rev. Lett. **80**, 5117 (1998).
- [7] A. A. Sukhorukov and Yu. S. Kivshar, Opt. Lett. **28**, 2345 (2003).
- [8] B. J. Eggleton *et al.*, Phys. Rev. Lett. **76**, 1627 (1996).
- [9] D. Mandelik *et al.*, Phys. Rev. Lett. **90**, 053902 (2003).
- [10] J. W. Fleischer *et al.*, Phys. Rev. Lett. **90**, 023902 (2003).
- [11] D. Neshev *et al.*, Opt. Lett. **28**, 710 (2003).
- [12] J. E. Sipe and H. G. Winful, Opt. Lett. **13**, 132 (1988).
- [13] J. Feng, Opt. Lett. **18**, 1302 (1993).
- [14] D. Mandelik *et al.*, Phys. Rev. Lett. **90**, 253902 (2003).
- [15] R. Morandotti *et al.*, Phys. Rev. Lett. **83**, 2726 (1999).